periodica polytechnica

Chemical Engineering
57/1–2 (2013) 79–83
doi: 10.3311/PPch.2174
http://periodicapolytechnica.org/ch

RESEARCH ARTICLE

Predicting the friction factor in straight pipes in the case of Bingham plastic and the power-law fluids by means of measurements and CFD simulation

Péter Csizmadia / *Csaba* Hős
Received 2012-11-05, accepted 2013-04-25

Abstract

In the petroleum, food and energy industry, non-Newtonian fluids are widely used and their transport in pipelines can be highly expensive. When designing such systems, predicting the pressure drop for a given flow rate is of primary importance. In this paper, the friction factor in straight pipelines is studied experimentally and by means of Computational Fluid Dynamics (CFD) techniques in the case of power-law and the Bingham plastic fluids. First, the accuracy of the CFD technique is demonstrated in the case of water. Then, a power-law fluid (Carbopol 971 solution) is examined experimentally and numerically and it is confirmed that by introducing the modified Reynolds number given in [1], *the classic friction factor formulae can be used. In the case of the Bingham plastic fluids, CFD simulations were performed and friction factor curves for several Hedström numbers are reported which were found to be consistent with the corresponding literature.*

Keywords

Bingham plastic fluid · Carbopol 971 solution · CFD simulation · friction factor · power-law fluid

Acknowledgement

The work reported in the paper has been developed in the framework of the project Talent care and cultivation in the scientific workshops of BME” project. This project is supported by the grant TÁMOP-4.2.2.B-10/1–2010-0009.

Péter Csizmadia
Department of Hydrodynamic Systems, Budapest University of Technology and Economics, Műegyetem rkp. 1., Budapest, H-1111, Hungary
e-mail: csizmadia@hds.bme.hu

Csaba Hős
Department of Hydrodynamic Systems, Budapest University of Technology and Economics, Műegyetem rkp. 1., Budapest, H-1111, Hungary
e-mail: hoscsaba@hds.bme.hu

1 Introduction

1.1 Motivation

Non-Newtonian fluids are widely encountered in industrial applications, for instance in coal-based power plants, food or petroleum industry. The transportation of these fluids is usually performed by pumping them via pipelines, in which – notably due to skin friction - pressure drop is observed. In the case of Newtonian fluids, this pressure loss depends primarily on the Reynolds number and on the roughness of the pipe (in the turbulent regime). However, in the case of non-Newtonian fluids, even defining the Reynolds number is not straightforward and introducing new parameters (such as the Hedström number) is also needed. When designing pipeline systems, one has to estimate the pressure losses to choose the suitable pumps and pipe diameters, which is often cumbersome due to the lack of experimental and theoretical guidelines. This study focuses on the possibility of employing Computational Fluid Dynamics (CFD) techniques for friction factor prediction of non-Newtonian fluids. We chose a simple, standard geometry (straight pipe). First, the accuracy of the CFD setup (mesh, turbulence model, etc.) is demonstrated in the case of water. Then, a power-law fluid (Carbopol 971 solution) is examined experimentally and numerically and it is confirmed that by introducing the modified Reynolds number given in [1], the classic friction factor formulae can be used. In the case of the Bingham plastic fluids, CFD simulations were performed and friction factor curves for several Hedström numbers are reported which were found to be consistent with the corresponding literature.

1.2 Literature overview

For purely viscous fluids (notably power law fluids), several experimental results can be found in the literature, see [1]–[7]. The most important results of these studies is that with the help of the modified Reynolds number (given by Equation (5)), the classic Moody diagram is applicable for such fluids. Moreover, the Poiseuille and Blasius correlations and the critical Reynolds number for laminar-turbulent flow remain valid.

In terms of Bingham plastic fluids, fewer studies were found. Reference [6] gives the Moody graph for Bingham plastic fluids,

Fig. 1. Rheology of (a) Carbopol 971 Solution, (b) Bingham plastic fluids. In both Figures water is shown by the red dash-dot line.

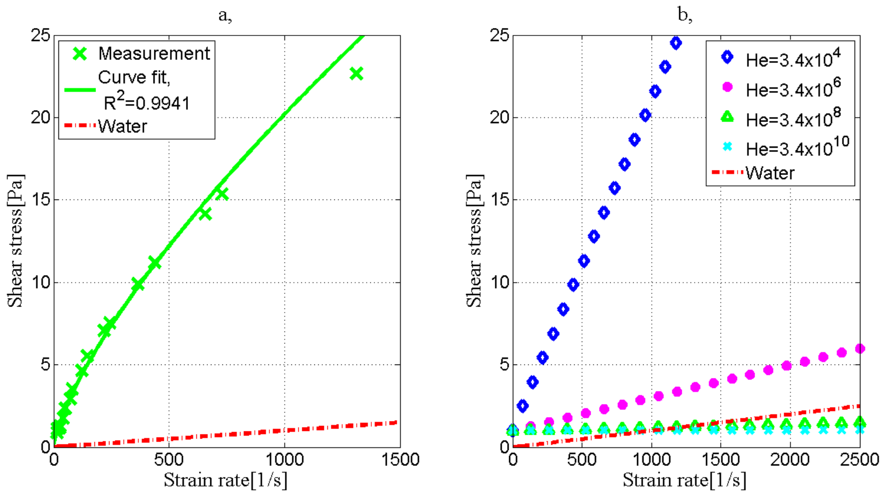

that shows that upon increasing the yield stress (Bingham number) the laminar segment is shifted right (i.e. the friction factor increases and the laminar-turbulent transition appears at higher Reynolds numbers). Reference [8] summarizes some aspects of the computational challenges when simulating Bingham flows. Explicit equations for several problems occurring in every-day engineering life are given in Reference [9]. References [10]–[12] summarize the analytical solutions and contain several experimental and numerical results.

The recent developments in CFD techniques allows the modelling of non-Newtonian flows and the prediction of flow losses, see [13]–[16] for such studies. However, it seems that the potential of CFD techniques is not fully exploited, probably mostly due to the uncertainties around the behaviour of the turbulence models in the case of non-Newtonian fluids.

2 Experimental

2.1 Carbopol 971 solution

In this part of the study, the material properties of the Carbopol 971 solution are presented. The rheological measurements were performed in the laboratory of Department of Hydrodynamic Systems. The analysed solution contains 0.13% Carbopol 971, 0.05% NaOH and 99.82% water. The NaOH was needed to set the pH-value to approximately 7. The measurement of the rheology was performed with a Rheotest 2 RV2 rotational viscosimeter. Figure 1.a presents the results of the rheological measurements and the curve fit of the shear stress-shear rate relationship described by

$$\tau = \mu_{PL}\dot{\gamma}^{n_{PL}} \tag{1}$$

with μ_{PL} consistency index and n_{PL} flow behaviour index (see e.g. [1] for details). The actual values are $\mu_{PL} = 0.1334$ [Pa s$^{n_{PL}}$] and $n_{PL} = 0.7266$ in our case.

2.2 Bingham plastic fluids

In the case of Bingham plastic fluids, the rheology can be described by

$$\tau = \tau_{\text{yield}} + \mu_B\dot{\gamma} \tag{2}$$

(again, see [1] for details) with μ_B viscosity consistency and τ_{yield} yield stress. In the case of Bingham plastic fluids, another important dimensionless number highlighting the importance of yield stress is the Hedström number, which is defined as (see [3])

$$He = \frac{D^2\rho\,\tau_{\text{yield}}}{\mu_B^2} \tag{3}$$

with D pipe diameter and ρ density. In the computations the pipe diameter, the density, and the yield stress were set to constant values, and the viscosity consistency was varied to perform the analysis at different Hedström numbers. Table 1 presents the typical values of these material and geometrical properties. In this case the Reynolds number, Re can be defined as (see [3] for details)

Tab. 1. Rheological and geometric properties of the examined models in the case of Bingham plastic fluids

D [m]	0.1	0.1	0.1	0.1
ρ [kg/m^3]	1370	1370	1370	1370
τ_{yield} [Pa]	1	1	1	1
μ_B[Pa s]	2×10^{-2}	2×10^{-3}	2×10^{-4}	2×10^{-5}
He [–]	3.4×10^4	3.4×10^6	3.4×10^8	3.4×10^{10}

$$Re = \frac{v\rho D}{\mu_B}. \tag{4}$$

Figure 1.b presents these rheological curves for different Hedström numbers. For comparison, both diagrams contain the rheology of water.

2.3 Experimental set-up

Figure 3 presents a sketch of the experimental set-up with the main elements. The test rig consists of a centrifugal pump (element 1), which pumps the fluid through the system from a tank. The flow rate was set by a control valve (element 2). Two pressure taps were mounted (p_1, p_2) to measure the pressure drop with the help of a multimanometer, in which the fluid was water. Before the first pressure tap, more than 15 diameters long (appr.

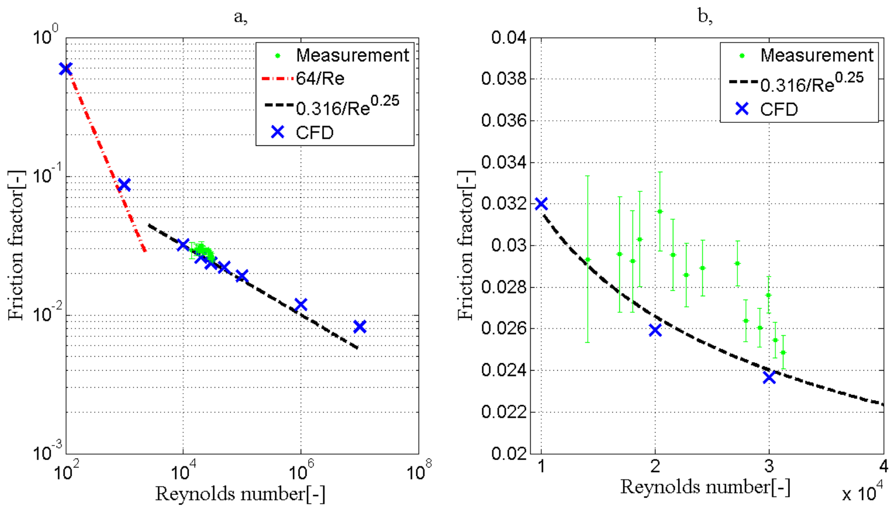

Fig. 2. (a) Validation of the CFD model (see Section 3 for details) and the measurements in the case of water. (b) A close-up of panel (a) highlighting the measured values.

310 mm) straight pipe was mounted to provide a fully developed velocity profile [17]. The system also contains a Venturi pipe (element 3) to measure the flow rate based on calibrated p(Q) curve. 20 millimetres was the inlet diameter and 298 millimetres was the length of the examined part of the pipe. The diameter of the vena contracta in the Venturi pipe was 11 millimetres where the pressure (p_4) was measured.

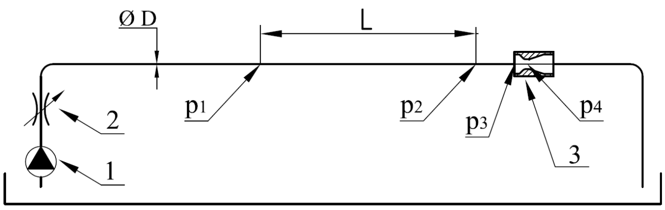

Fig. 3. The sketch of the experimental set-up.

2.4 Validation

As a first step, both the CFD technique and the test rig were validated with the help of the theoretical results of the friction factor of the water, which is well-known from the literature [2]. Figure 2.a presents the friction factor in a wide range of Reynolds number for water. The red dash-dot line shows the *64/Re* correlation (laminar case, $Re < 2300$) and the black dashed line presents the Blasius equation $0.316/Re^{0.25}$ (turbulent case, $Re > 2300$). A good agreement can be observed in the case of the numerical results, which is marked by the blue crosses. The measurements were performed between Reynolds number range of 10 000 and 30 000, which are shown by the green dots with the error bars, Figure 2.b. As it can be seen, both techniques gave fairly close results thus judged to be reliable enough for further computations. The slightly higher values in the case of the measurements are due to the fact that the measured pipe was not hydraulically smooth.

3 CFD set-up

A fully structured grid was built with the help of ICEM CFD, consisting of approximately 32 000 elements. This spatial resolution was found to be suitable to obtain grid-independent solutions (see Figure 2). Due to the axisymmetry, only 10 degrees were modelled and periodicity was prescribed which allowed the drastic decrease of the problem size (purple arrows in Figure 4). The length of the pipe was 10 meter, which was found to be long enough to develop a proper velocity profile.

Ansys CFX 13.0 was used as flow solver, steady state computations were performed. High-resolution spatial scheme was used for all of the equations, except for the turbulence model, for which first-order numerics was set. The actual turbulence model was the SST model. One computation typically needed approx. 5000–25000 iteration steps and about 5–15 hours on a standard desktop PC (3.4 GHz CPU, 4 GB RAM) depending on the Reynolds number and the material properties. In most of the computations, the auto timescale option of CFX (that detects automatically the suitable time step) was sufficient for convergence, however, beyond $He = 10^3$ the local timescale option was needed for stable computations (for details, see [18]).

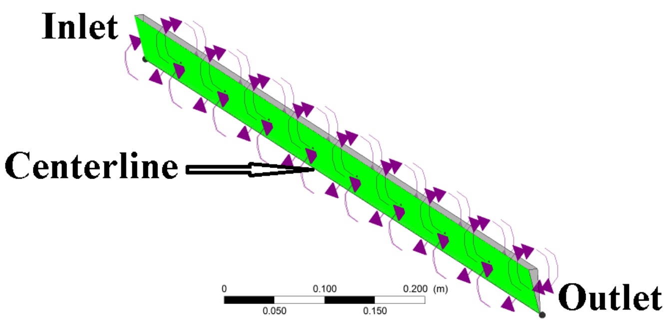

Fig. 4. The sketch of the CFD model

4 Results and their discussion

4.1 Power-law fluid

Figure 5. presents the friction factor in the case of the Carbopol 971 solution as a function of the generalized Reynolds number Re_{PL} (see [1] for details), defined as

$$Re_{PL} = v^{2-n_{PL}} D^{n_{PL}} \rho \left[\mu_{PL} 8^{n_{PL}-1} \left(\frac{1+3n_{PL}}{4n_{PL}} \right)^{n_{PL}} \right]^{-1} \tag{5}$$

Fig. 5. Friction factor in the case of the Carbopol 971 solution with generalized Reynolds number [1].

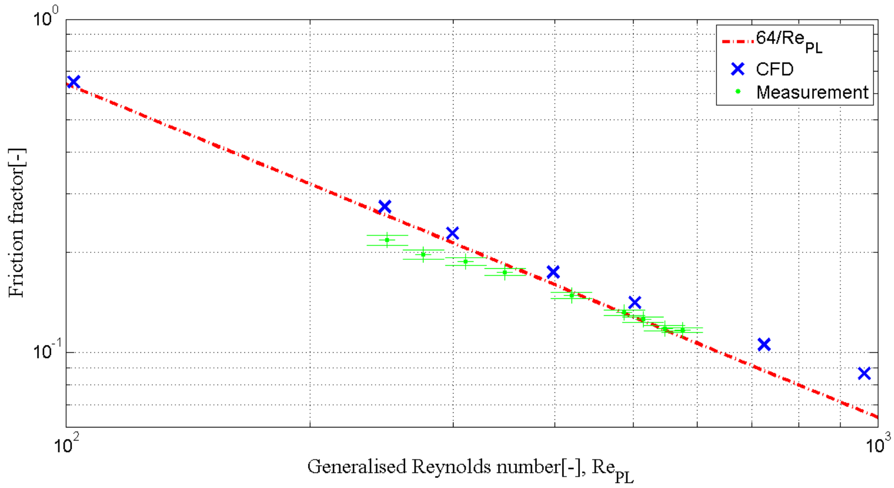

Fig. 6. Friction factor in the case of the Bingham plastic fluids for different Hedström numbers

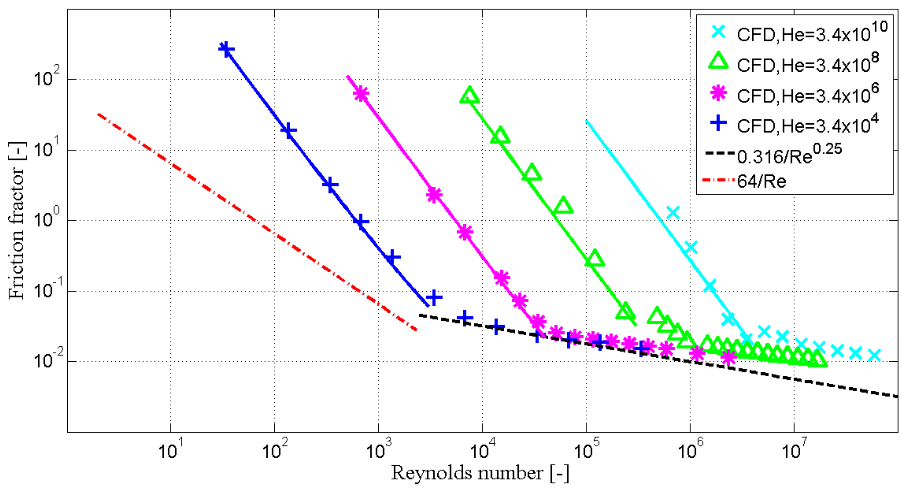

with v average velocity. As it can be seen this extension of the Reynolds number allows the usage of the classic formulae in the laminar case. The red dash-dot line shows the *64/Re* law, the green points with the error bars present the results of the measurements while the CFD results are denoted by the blue crosses.

4.2 Bingham plastic fluid

In Figure 6, the friction factors are presented for several Hedström numbers as a function of the Reynolds number. The red dash-dot line shows the *64/Re* law, and the black dashed line presents the Blasius correlation $0.316/Re^{0.25}$. CFD simulations were performed with different μ_B viscosity consistency values which imply different rheology, as it was mentioned in Figure 1.b and Table 1. The solid lines, which are valid in the laminar case, are calculated from the Buckingham-Reiner equation [19]

$$f = \frac{64}{Re}\left[1 + \frac{He}{6Re} - \frac{64}{3}\left(\frac{He^4}{f^3 Re^7}\right)\right], \tag{6}$$

which was simplified by [9] to the following explicit form:

$$f = \frac{64}{Re} + \frac{10.67 + 0.1414(He/Re)^{1.143}}{[1 + 0.0149(He/Re)^{1.16}]Re}\left(\frac{He}{Re}\right) \tag{7}$$

It can be observed, that the Newtonian form is regained in the case of the $He = 0$.

Figure 6 depicts the friction factor for the Bingham plastic fluid case for several Hedström numbers. As it can be seen, the CFD results agree with theory not only qualitatively but also quantitatively, that is, they capture the shift of the laminar regime towards higher Reynolds numbers with increasing Hedström number. Moreover, the numerical technique seems to give reasonable values also in the turbulent regime, where slightly higher values are observed than the Blasius equation. Similar result was reported in [19].

5 Conclusions

In this study, the prediction of the friction factor in straight pipelines was presented in the case of the Carbopol 971 power law solution and the Bingham fluids. The first fluid was analysed with experimental and numerical method (CFD) and the second one was examined with the help of CFD, both models were validated. This study also contains the rheology of these non-Newtonian fluids. The presented results show a fairly good agreement with the available literature, meaning that CFD techniques seem to be mature enough nowadays to predict fluid losses for non-Newtonian fluid with standard turbulence models.

References

1 **Monteiro ACS, Bansal PK**, *Pressure drop characteristics and rheological modeling of ice slurry flow in pipes*, International Journal of Refrigeration, **33**(8), (December 2010), 1523–1532.

2 **Tamás L**, *Basics of fluid mechanics*, Műegyetem Kiadó; Budapest, 2008 (in Hungarian).

3 **Grozdek M, Khodabandeh R, Lundqvist P**, *Experimental investigation of ice slurry flow pressure drop in horizontal tubes*, Experimental Thermal and Fluid Science, **33**(2), (January 2009), 357–370.

4 **Kitanovski A, Vuarnoz D, Ata-Caesar D, Egolf PW, Hansen TM, Doetsch C**, *The fluid dynamics of ice slurry*, International Journal of Refrigeration, **28**(1), (January 2005), 37–50.

5 **Etemad SG**, *Turbulent Flow Friction Loss Coefficients of Fittings for Purely Viscous Non-Newtonian Fluids*, International Communications in Heat and Mass Transfer, **31**(5), (July 2004), 763–771.

6 **Chhabra RP, Richardson JF**, *Non-Newtonian flow and applied rheology*, Elsevier, 2008.

7 **Meng L, Zhang M, Shen L**, *Study on the resistance properties of pumping coal-water paste in pipes*, Chemical Engineering Science, **55**(15), (1 August 2000), 3053–3056.

8 **Dean EJ, Glowinski R, Guidoboni G**, *On the numerical simulation of Bingham visco-plastic flow: Old and new results*, Journal of Non-Newtonian Fluid Mechanics, **142**(1–3), (16 March 2007), 36–62.

9 **Swamee PK, Aggarwal N, Guidoboni G**, *Explicit equations for laminar flow of Bingham plastic fluids*, Journal of Petroleum Science and Engineering, **76**(3–4), (March 2011), 178–184.

10 **Bird RB, Stewart WE, Lightfoot EN**, *Transport Phenomena*, Wiley Book Co.; New York, 1960.

11 **Hallbom DJ**, *Pipe Flow of Homogeneous Slurry*, PhD Thesis; Vancouver, 2008.

12 **Haldenwang R, et al.**, *Sludge pipe flow pressure drop prediction using composite power-law friction factor-Reynolds number correlations based on different non-Newtonian Reynolds numbers*, Water SA, **38**(4), (July 2012).

13 **Gertzos KP, Nikolakopoulos PG, Papadopoulos CA**, *CFD analysis of journal bearing hydrodynamic lubrication by Bingham lubricant*, Tribology International, **41**(12), (December 2008), 1190–1204.

14 **Eesa M, Barigou M, Papadopoulos CA**, *FD analysis of viscous non-Newtonian flow under the influence of a superimposed rotational vibration*, Computers & Fluids, **37**(1), (January 2008), 24–34.

15 **Tsangaris S, Nikas C, Tsangaris G, Neofytou P**, *Couette flow of a Bingham plastic in a channel with equally porous parallel walls*, Journal of Non-Newtonian Fluid Mechanics, **144**(1), (June 2007), 42–48.

16 **Niezgoda-Żelasko B, Zalewski W**, *Momentum transfer of ice slurry flows in tubes, modeling*, International Journal of Refrigeration, **29**(3), (May 2006), 429–436.

17 *Measurement of fluid flow by means of pressure differential devices inserted in circular cross-section conduits running full - Part 1: General principles and requirements*, 1995, Standard No.:MSZ ISO 5167-1.

18 *ANSYS CFX-Solver Theory Guide*, Release 13.0, ANSYS, Inc.

19 **Darby R, Melson J**, *How to predict the friction factor for flow of Bingham plastics*, Chem. Eng., **28**, (1981), 59–61.